FIFTH AUSTRALASIAN CONFERENCE

on

HYDRAULICS AND FLUID MECHANICS

at

University of Canterbury, Christchurch, New Zealand

THE DYNAMICS OF VAPOUR BUBBLES ATTACHED TO INCLINED HEATED SURFACES IN A FLOW MEDIUM

by

J. G. SYMONS B.E., S.I.E. Aust.

S. E. BONAMY B.E., M.Sc., Ph.D., A.S.T.C.
F.I.Mech.E., F.I.E. Aust.

SUMMARY

The cooling capacity of a convective flow field around an inclined surface is examined for varying surface inclinations. It is shown that the flow medium influences, to a large degree, the cooling capacity of the system.

Hydrodynamic effects acting on a vapour nucleus, together with the growth of a thermal layer is investigated to predict bubble waiting period. Bubble growth rate is studied theoretically by considering the effects of pressure, surface tension and viscosity, and a subsequent mathematical model developed to include effects of the thermal boundary layer. Shape variation of vapour bubbles is observed during growth and for different inclinations of the heating surface.

A maximum bubble diameter model is presented, by considering a bubble force balance introduced by hydrodynamic effects.

J. G. SYMONS Research Student, School of Civil, Mechanical and Mining Engineering
Wollongong University College. Australia.

S. E. BONAMY Acting Head, School of Civil, Mechanical and Mining Engineering
Wollongong University College. Australia.

Nomenclature

a	-	Thermal diffusivity
C_D	-	Drag coefficient
D_D	-	Departure diameter
e	-	Extension tube length
F	-	Indicated F stop
F_e	-	Effective F stop
f	-	Bubble departure frequency
f_e	-	Focal length of lens
g_c	-	Gravitational constant
h_{fg}	-	Specific heat of vaporisation
K	-	Constant
K_1, K_2	-	Area factors, fig. 6
k	-	Thermal conductivity
ℓ	-	Thickness of heating strip
N_B	-	Bouyant force
N_D	-	Flow medium drag
N_G	-	Bubble growth force
N_P	-	Pressure force
$N_{S.T.}$	-	Surface tension force
P	-	Pressure
P'	-	Inert gas partial pressure
R	-	Bubble radius
R_c	-	Nucleating cavity radius
R_I	-	Initial bubble radius
S	-	Bubble shape factor, fig. 9
T	-	Temperature
t	-	Time
u	-	Flow medium velocity
v	-	Specific volume
δ	-	Superheated layer thickness
θ	-	Heated surface inclination
υ	-	Kinematic viscosity
ρ	-	Density
σ	-	Surface tension
ϕ	-	Heat flux

Subscripts

I	-	Insulated face of heating strip
ℓ	-	Liquid
N	-	Nichrome V
R	-	Vapour-liquid interface
SAT	-	Saturation (temperature)
v	-	Vapour
w	-	Boiling surface
∞	-	Bulk liquid

Introduction

The dynamics of vapour bubbles in two-phase flow has long been of interest to the engineer mainly because it provides a means of rapid energy transport from a surface to a fluid. It has been of particular interest not only in relation to boiling phenomena associated with steam generation, refrigeration and air-conditioning, but also, more recently, in cooling related to rocket nozzles and nuclear reactors. The boiling phenomena is not as yet well understood, although in recent years, research has been conducted in many countries with moderate success.

In much of the work on this topic, simplifications have been introduced by studying heat and mass transfer from heated horizontal surfaces in tanks of initially stagnant liquid. However, even in such studies, commonly referred to as "Pool Boiling", the subsequent convection currents generated introduce fluid flow effects which can never be completely eliminated. Thus a complete analysis must include a simultaneous examination of fluid flow, heat transfer and thermodynamic effects. In this respect, a research programme is described here in which theoretical models have been developed to simulate the boiling mechanism. It applies to all inclines of a heated surface and the subsequent prediction of bubble parameters is made. The theoretical results are compared with data collected from an experimental test rig in which high speed photography and shadow techniques were used.

Experimental Equipment

The experimental equipment comprised a brass tank containing distilled water, with hardened

glass windows on the front and rear (Fig. 1). The heating surface, nichrome V (Ref. 1), was clamped to brass electrodes and cast in high temperature araldite to provide thermal insulation for the back of the strip. This arrangement provided a single heating surface of 50.8 mm x 6.35 mm exposed to the distilled water. A copper-constantan thermocouple was spot welded to the back of the heating strip and connected to a potentiometer. Errors due to heat conduction along the thermocouple wires (Ref. 2) were minimised by using fine wire (30 gauge), insulated with enamel, glass and a compound which was resistant to both moisture and heat.

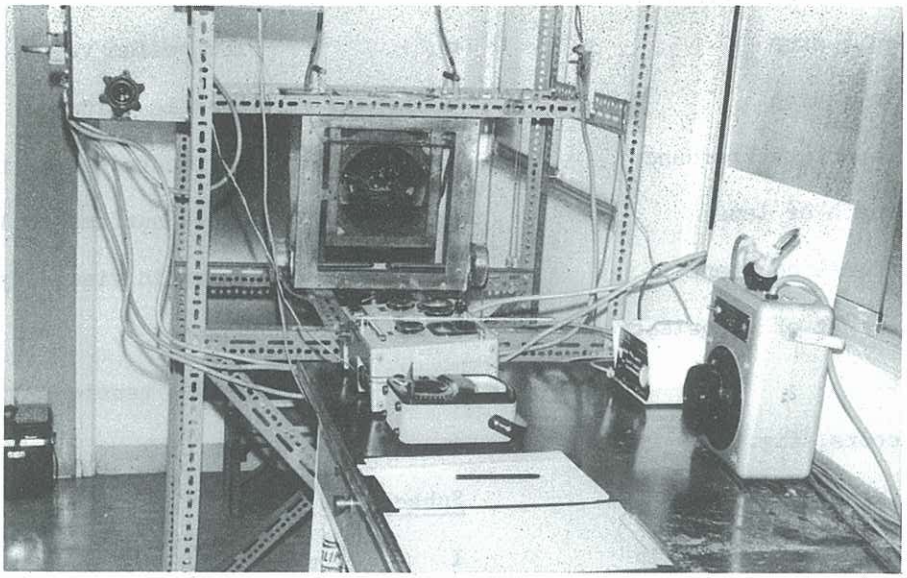

FIG. 1 EXPERIMENTAL EQUIPMENT

Direct current heating of the test surface was supplied from 6 volt, 200 amp-hour lead-acid batteries. The D.C. heating eliminated temperature fluctuations and thermocouple pickup which is normally experienced with A.C. heating (Ref. 3). Continuous current control from 0 to 100 amps was achieved with a resistance bank consisting of a carbon plate rheostat, together with a parallel arrangement of fixed resistances. The power delivered to the surface was measured with a voltmeter and shunted ammeter.

Thermocouple errors due to electric heating of the test surface were eliminated by taking temperature readings for both polarities, a two pole reversing switch being provided for this purpose. The boiling surface temperature, T_W, was calculated from the thermocouple reading of the insulated face, T_I, by assuming one-dimensional heat transfer across the nichrome V strip.

$$T_W = T_I - \frac{\phi_W \ell}{2 k_N} \qquad \ldots (1)$$

The test surface and electrodes were mounted on an angularly graduated annulus to allow inclination of the test block without changing heat flux and maintaining the centre of the surface at a constant liquid depth. The bulk liquid temperature, maintained at 100°C, was measured at various localities with copper constantan thermocouples and a digital thermocouple indicator. Bulk heating and temperature control of the liquid was achieved using a variac and two 900 watt immersion heaters.

Photographic Techniques

A shadow technique was used to photograph the bubbles, providing a sharp contrast and fine resolution between the vapour and liquid. A 1 Kw Quartz Halogen light source was directed through the tank directly into the camera lens. Lens sheeting was placed between the Quartz Halogen light and the tank to diffuse the light and provide a screen of uniform illumination. Two filament lights, each of 500 watts were placed on the same side of the tank as the camera, and directed back through the boiling water toward the illuminated screen (Fig. 2). Using this arrangement, the light passed freely through the undisturbed liquid providing a white area on the reversal processed film. When a vapour bubble came between the lens and illuminating screen,

light was deflected at the vapour-liquid interface leaving a black void on the film. One frame of the film has been included in Fig. 3.

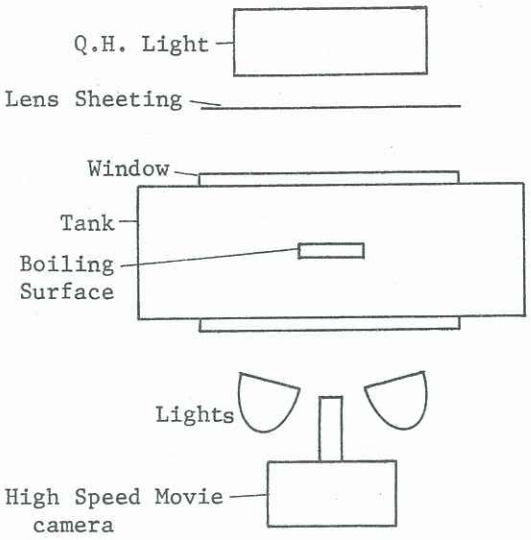

FIG. 2 PHOTOGRAPHIC ARRANGEMENT

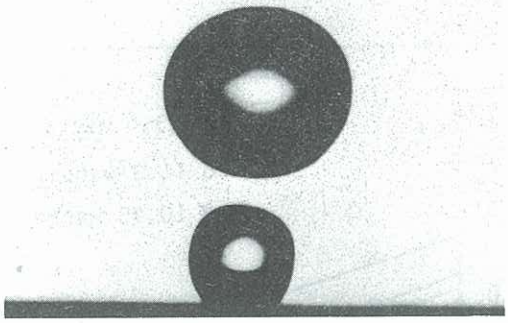

FIG. 3 ONE FRAME OF HIGH SPEED FILM

A Hycam movie camera with 1:4/150 mm lens, together with 96 mm of extension tubes allowed a viewing area of 13.5 mm x 8.5 mm to be recorded on film. The lens aperture indicated by a light meter reading, F, was corrected for lens extension to yield an effective aperture, F_e, from the correction equation :

$$F_e = F\left(\frac{f_\ell + e}{f_\ell}\right) \qquad \ldots (2)$$

For a framing rate of 2500 frames per second, the required aperture was 1/4.5 using 16 mm Tri-X cine reversal film. A timing light generator recording timing marks on the film at a known frequency of 100 Hz allowed precise calculation of the time increment between each film frame.

Experimental Procedure

The test surface was prepared with 600 grit emery paper until the surface was smooth, all rubbings being parallel to the axis of the strip. The distilled water was boiled for 1 hour to degas the system, and after the required surface temperature was set, a further 30 minutes was allowed for the system to stabilise.

In the tests which involved high speed photography, an artificial nucleating site was established by drilling a 0.356 mm diameter hole in the surface. Film was exposed in 30 metre lengths for surface inclinations of $\theta = 0°$ (heating surface horizontal and facing upwards), 45°, 90° (vertical), 135° and 180° (horizontal facing downwards). The surface temperature was adjusted to 103°C between each exposure and 30 minutes allowed before starting the next test.

The processed films were analysed using a 16 mm micro-film reader which provided an overall magnification of 15.3 over the original bubble size.

Cooling Capacity

To study the cooling capacity of boiling within a flow medium which is induced solely by the system, all external convection currents had to be shielded from the heating surface. A perspex housing was used to allow free movement of internal two phase flow induced by the boiling surface, with excess vapour escaping to the bulk liquid, and preventing effects due to external convection currents induced by the immersion heaters .

Under these conditions, tests were performed by measuring the excess temperature required to maintain a given rate of energy transfer at each surface inclination. The results of the three

tests performed at constant heat fluxes are illustrated in Fig. 4. This shows that increased exposure to the induced flow medium, θ increasing, substantially increases the energy transport efficiency. A much smaller surface temperature is required to provide the same rate of heat transfer for large surface inclinations. The effect can be illustrated further by examining the temperature profiles near the boiling surface as shown in Fig. 5 again with the perspex shielding in place. For larger values of θ, the cooler bulk liquid penetrates closer to the heating surface, and the corresponding reduction in thickness of the superheated liquid layer allows increased heat exchange.

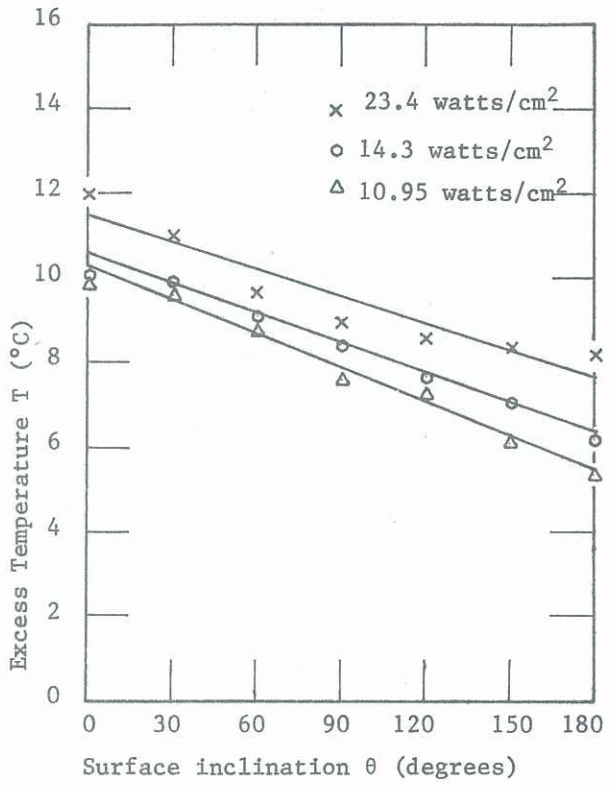

FIG. 4 REQUIRED EXCESS TEMPERATURE

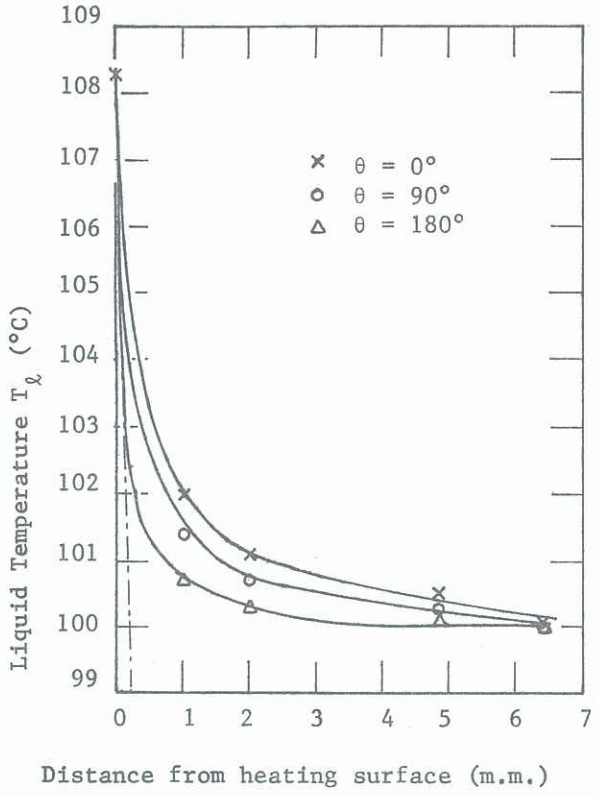

FIG. 5 TEMPERATURE PROFILES

Bubble Waiting Period

The waiting period is the time from departure of one vapour bubble to the beginning of growth of the next. When the vapour mass departs the heated surface, it carries with it a superheated liquid layer. The volume previously occupied by its vapour is then replaced with cooler liquid and a finite time is required for the liquid temperature to rise to that required for incipience of boiling.

By considering equilibrium across the liquid-vapour interface, together with the Clausius-Clapeyron equation, it can be shown that the vapour temperature required for a spherical nucleus to grow is (Ref. 4)

$$T_v = T_{sat} + \frac{2 \sigma T_{sat} v_v}{h_{fg} R} \qquad \ldots (3)$$

During the waiting period, the increase in liquid temperature with time can be found by considering a one dimensional heat conduction from the heated surface to the bulk liquid. Boundary conditions assume that the inflowing liquid is initially at temperature $T_\ell = T_\infty$, giving the equation developed by Carslaw and Jaeger (Ref. 5).

$$T = T_\infty + \frac{2 \phi_W (a t)^{\frac{1}{2}}}{k} \sum_0^\infty (-1)^n \left[\text{ierfc} \frac{(2n+1)\delta - x}{2(a t)^{\frac{1}{2}}} - \text{ierfc} \frac{(2n+1)\delta + x}{2(a t)^{\frac{1}{2}}} \right] \qquad \ldots (4)$$

It can be assumed that a bubble will begin to grow when the surrounding liquid has increased to a temperature which is equal to or greater than the vapour temperature T_v, i.e. when the liquid at the extreme of the bubble reaches a temperature given by equation 3. For this model the waiting period is calculated by assuming $T = T_v$ and equating equations 3 and 4. When $\theta = 180°$ the assumption that initially $T_\ell = T_\infty$ is most closely met for all surface inclinations because liquid temperature is the coolest for this inclination (Fig. 5). From data obtained by the high speed photography, the waiting period was found to be 13.6 milli-seconds compared with 12 milli-seconds as obtained from the theoretical equations 3 and 4. For smaller values of θ, the incoming liquid temperature is progressively higher, allowing the liquid temperature to reach the equilibrium requirement much sooner. This gives smaller waiting periods for smaller values of θ, as was verified experimentally (Table 1). The theoretical determination of waiting period for other inclinations can be achieved only if the temperature of incoming liquid is known.

TABLE I - EXPERIMENTAL DATA

SURFACE INCLINATION θ, (degrees)	HEAT FLUX ϕ, (watts/cm^2)	WAITING PERIOD (milli-seconds)	GROWTH PERIOD (milli-seconds)	DEPARTURE RADIUS (mm)
0	.87	0	41.7	1.36
45	.98	0	39.7	1.27
90	1.08	.6	26.8	.99
135	1.38	8.4	57.8	.97
180	1.65	13.6	-	-

Bubble Growth

The first analysis of bubble growth was performed by Lord Rayleigh (Ref. 6). He studied pressure effects due to collapsing spherical cavities in an incompressible liquid and obtained the relation

$$\frac{\rho_\ell}{g_c}\left(R\ddot{R} + \frac{3}{2}\dot{R}^2\right) = P_{\ell,R} - P_{\ell,\infty} \qquad \ldots (5)$$

In his derivation, Rayleigh assumed $P_{\ell,R} - P_{\ell,\infty}$ = constant. However, by considering the pressure differential across the bubble interface due to surface tension, a modified or extended Rayleigh Equation gives

$$\frac{\rho_\ell}{g_c}\left(R\ddot{R} + \frac{3}{2}\dot{R}^2\right) = P_v - P_{\ell,\infty} - \frac{2\sigma}{R} \qquad \ldots (6)$$

A further improvement on the Rayleigh Equation considering liquid viscosity and gas inclusion (Ref. 7) yields

$$\frac{\rho_\ell}{g_c}\left(R\ddot{R} + \frac{3}{2}\dot{R}^2 + \frac{4\upsilon}{R}\dot{R}\right) = P_v + P' - P_{\ell,\infty} - \frac{2\sigma}{R} \qquad \ldots (7)$$

Equations (5), (6), and (7) have been solved numerically using a seven term Taylor Series Expansion with initial conditions duplicating the high speed photography tests. The results from subsequent computer programmes are compared with growth rates obtained by high speed photography in Table 2.

The theoretical equations illustrate the degree of restriction placed on bubble growth by surface tension and liquid viscosity. Also, they predict growth rates far in excess of those actually observed, with identical growth rates for all inclinations of the heated surface. In the derivation of the three equations it has been assumed that bubble growth is limited only by pressure, surface tension and liquid viscosity. These assumptions are valid for very early stages of growth, however, as the bubble becomes visible, growth is dependent also on evaporation

of the liquid-vapour interface. The rate of evaporation is in turn dependent on energy transport into the bubble, a factor which has been neglected in the previous equations.

TABLE 2 - COMPARISON OF GROWTH THEORIES

TIME	RADIUS (m.m.)			
(micro-sec)	Equation 5	Equation 6	Equation 7	Experimental
0	.24	.24	.24	.24
30	1.76	1.75	1.74	-
60	3.42	3.4	3.39	-
90	5.08	5.05	5.03	-
110	6.18	6.16	6.15	-
400	-	-	-	.29
900	-	-	-	.35

The energy transport into a bubble, which is covered with a superheated liquid layer, is allowed for by considering one dimensional heat conduction across the thermal layer, together with area factors for different surface inclinations, (Fig. 6). The heat conduction across the superheated layer into the bubble is given by

$$\frac{\partial T}{\partial t} = a \frac{\partial^2 T}{\partial x^2} \qquad \ldots (8)$$

with boundary conditions

$$T(t,o) = T_\infty, \quad T(t,\delta) = T_v, \quad T(o,x) = \frac{\phi_w x}{k}.$$

By summing the energy transfer across the vapour-liquid interface, and into the bubble base, the resulting equation is

$$R = R_I t' + \left(\frac{K_1}{K_2} - \frac{(T_v - T_\infty) k \pi}{2 \delta K_2 \phi_w} \right)(1-t') + \sum_{1}^{\infty} \frac{\pi \left(\phi_w - \frac{k(T_v - T_\infty)}{\delta}\right)}{K_2 \phi_w - \frac{a n^2 \pi^2 h_{fg} \rho_v}{\delta^2}} \left(\mathrm{EXP}\left(- \frac{a n^2 \pi^2 t}{\delta^2} \right) - t' \right) \qquad \ldots (9)$$

where $t' = \mathrm{EXP}\left(- \frac{K_2 \phi_w t}{h_{fg} \rho_v} \right)$.

The experimental bubble growth for each surface inclination is illustrated in Fig. 7. For one particular inclination, the vapour growth is compared with that predicted from equations 5, 6, 7 and 9 in Fig. 8. It is found that the diffusion controlled bubble growth model, equation 9, predicts vapour growth for all surface inclinations with acceptable accuracy. In the development of the model, a linear temperature profile was assumed (dashed line of Fig. 5). As the bubble grows beyond the thermal layer the surrounding liquid is slightly warmer than the assumed value of T_∞. For large bubble diameters, the model would predict growth rates which are slightly smaller than those actually observed (Fig. 8).

Bubble Shape

The changing bubble shape with time for each inclination is illustrated in Fig. 9, where the the ratio of bubble dimensions parallel and perpendicular to the heating surface is represented by a bubble shape factor S. The initial shape is seen to be strongly influenced by the amount of vapour retracting to the nucleating site after departure of the previous bubble. During growth the vapour assumes a near spherical shape due to surface tension, although as the volume and projected area become appreciable, drag and bouyancy tend to elongate the bubble vertically for $\theta = 0°$, and flatten it over the surface at $\theta = 180°$. For inclinations between the two extremes, the vapour is attached to the cavity on its lower side and distorted upwards.

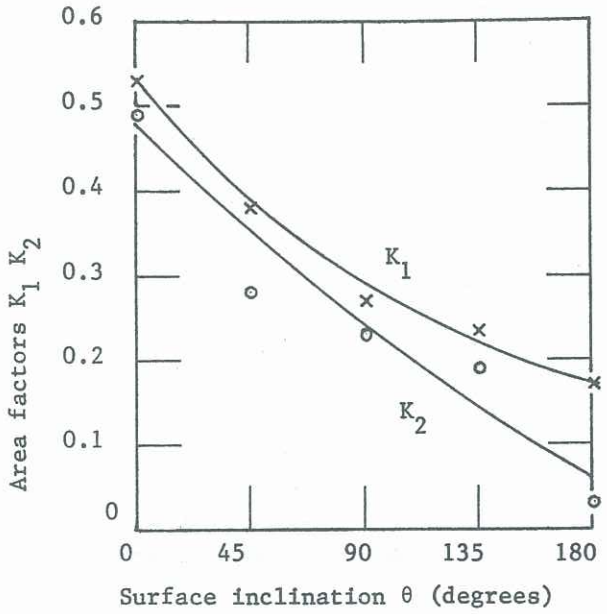

FIG. 6 AREA FACTORS

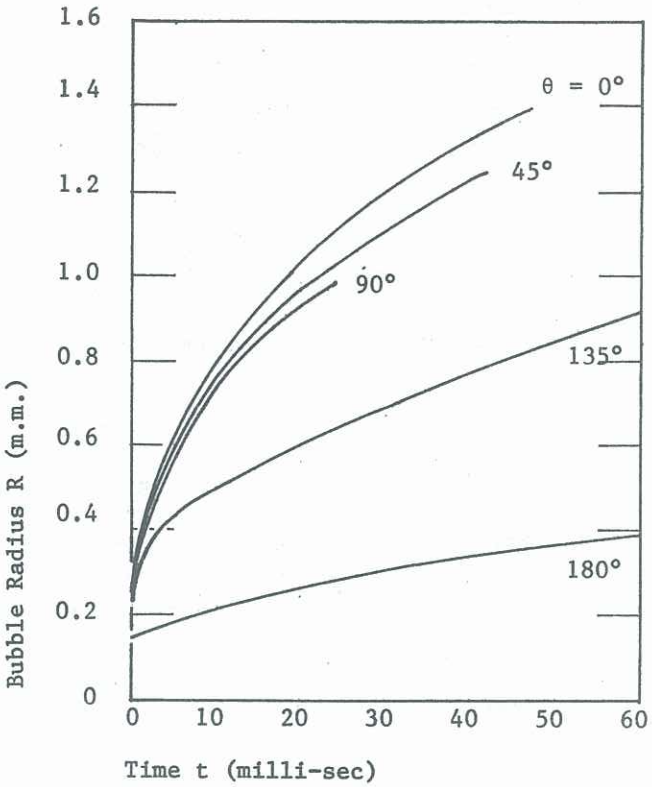

FIG. 7 VAPOUR BUBBLE GROWTH

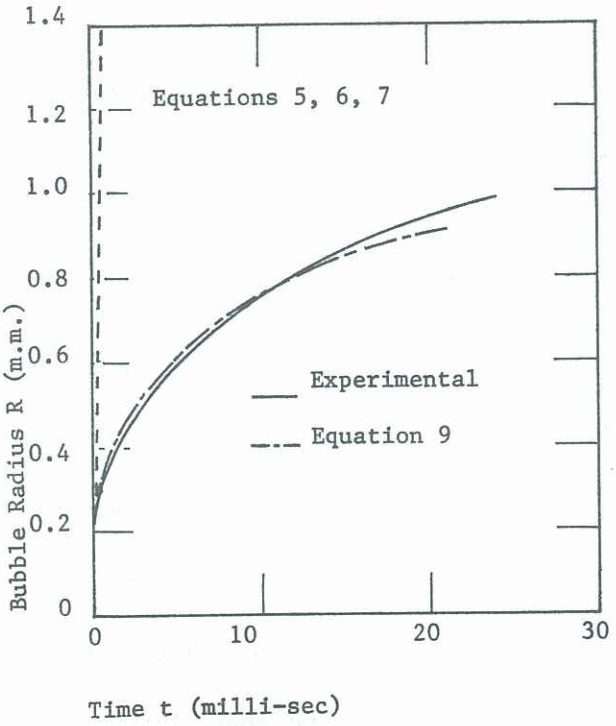

FIG. 8 COMPARISON OF BUBBLE GROWTH THEORIES, θ = 90°

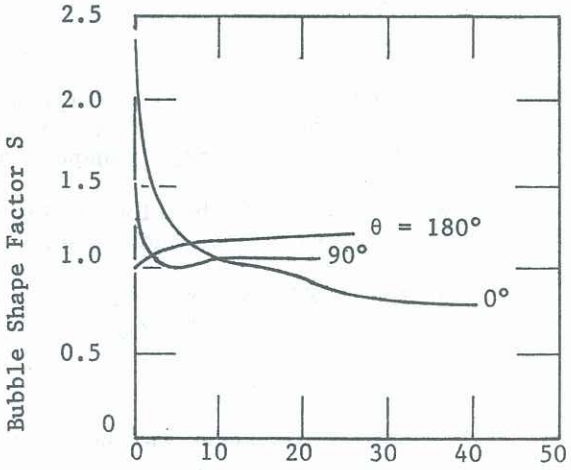

FIG. 9 BUBBLE SHAPE

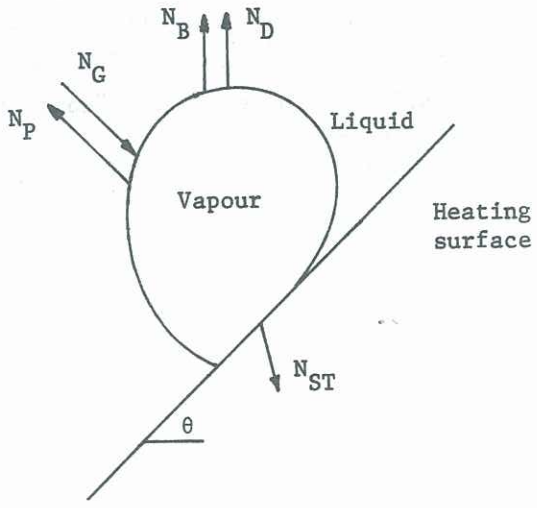

FIG. 10 BUBBLE DEPARTURE FORCE MODEL

Departure Diameter

By considering the departure model of Fig. 10, a prediction can be made of the diameter of a bubble leaving the heated surface.

Just prior to departure, the significant forces acting on it are as follows :-

Bouyancy $$N_B = (\rho_\ell - \rho_v)\, g\, \frac{4}{3}\, \pi\, R^3 \quad \ldots (10)$$

Flow Medium Drag $$N_D = 0.5\, \rho_v\, u^2\, C_D\, \pi\, R^2 \quad \ldots (11)$$

Interface Pressure Difference $$N_P = \frac{2\, \sigma\, \pi\, R_c^{\,2}}{R} \quad \ldots (12)$$

Bubble Growth $$N_G = 2\, \rho_\ell\, \dot{R}^2\, C_D\, \pi\, R^2 \quad \ldots (13)$$

Surface Tension $$N_{S.T.} = 2\, \sigma\, \pi\, R_c \quad \ldots (14)$$

By summing the forces acting on the model as outlined above, the maximum bubble diameter was calculated for $\theta = 0°$ and $90°$. The computed diameters were 2.28 and 1.82 mm, compared with experimental values of 2.72 and 1.98 mm respectively.

It should be noted that for $\theta = 180°$ a departure diameter does not exist because the vapour slides from the surface and does not experience the snapping action that takes place with all other inclinations.

Conclusion

If a heated surface, which induces boiling within a flow medium, is varied in inclination to increase the vapour exposure to the flow, the cooling capacity of the system is substantially increased.

The corresponding variations in temperature profiles determine the growth rate of vapour bubbles generated on the surface. The rate of growth of vapour can be determined theoretically by calculating the rate of energy transport across the vapour-liquid interface.

Temperature profiles of the flow medium control the bubble waiting period which is found to increase as surface inclination increases.

The diameter of bubbles departing the heated surface can be predicted by considering a hydrodynamic force balance on the vapour.

References

1. Nickel-Chronium Resistance Heating Alloys. British Driver - Harris. Data Sheet No. 5.
2. Howell, J.R. and Siegel, R. "Incipience, Growth and Detachment of Boiling Bubbles in Saturated Water from Artificial Nucleation Sights of Known Geometry and Size". International Heat Transfer Conference, Vol. 1966 p 12-23.
3. Moore, F.D. and Mesler, R.B. "The Measurement of Rapid Surface Temperature Fluctuation During Nucleate Boiling of Water". A.I.Ch.E. Journal. December 1961, p 520-624.
4. Tong, L.S. "Boiling Heat Transfer and Two-Phase Flow". John Wiley and Sons, Inc. p 7.
5. Carslaw, H.S. and Jaeger, J.C. "Conduction of Heat in Solids". Second Edition University Press (Oxford) 1959.
6. Rayleigh, Lord "On the Pressure collapse of a spherical cavity". Phil. Mag. 34, p 94 - 98 (1917).
7. Bankoff, S.G. "Diffusion Controlled Bubble Growth". Advances in Chemical Engineering, 6, p 1-60, 1966.